Journal of Statistical Physics, Vol. 83, Nos. 1/2, 1996

Scars in Nonintegrable and Rational Billiards

M. Tomiya[1] and N. Yoshinaga[2]

Received January 4, 1995; final October 26, 1995

We numerically study quantum mechanical features of the Bunimovich stadium billiard and the rational billiards which approach the former as the number of their sides increases. The statistics of energy levels and eigenfunctions of the rational billiards becomes indistinguishable from that of the Bunimovich stadium billiard below a certain energy. This fact contradicts the classical picture in which the Bunimovich stadium billiard is chaotic, but the rational billiard is pseudointegrable. It is numerically confirmed that the wave functions do not detect the fine structure, which is much smaller than the wavelength.

KEY WORDS: Quantum chaos; pseudointegrable systems; Bunimovich stadium; rational billiard.

1. INTRODUCTION

Integrable systems are exceptional in dynamical systems, while systems which are rigorously proved to be chaotic are also rare. This is partly due to the inevitable mathematical complexity of the proofs (e.g., the Sinai billiard and the Bunimovich stadium). However, there exists a wide intermediate range of dynamical systems which are neither integrable nor chaotic. The pseudointegrable system[1] is one such system, which has n degrees of freedom and n constants of motion as the integrable system has, but its variables are not separable. The pseudointegrable system differs from the integrable one in that its constants of motion do not make an invariant torus in phase space. If they make a torus, each degree of freedom is connected to a global constant of motion and the system becomes integrable.

[1] Department of Applied Physics, Faculty of Engineering, Seikei University, Kichijoji-Kitamachi 3-3-1, Musashinoshi, Tokyo 180, Japan.

[2] Department of Physics, Faculty of Science, Saitama University, Shimo-okubo 255, Urawashi, Saitama 338, Japan.

0022-4715/96/0400-0215$09.50/0

The rational billiard is different from the ordinary stadium billiard in that the latter's semicircular parts are replaced by polygons. The rational billiard is an example of pseudointegrable systems.[2–4] Recently in classical mechanics it has been reported that even the rational billiard shows some chaotic features like the Bunimovich stadium if it has sufficiently many sides.[5] It has been argued that the Lyapunov exponents are crucially dependent on the "precision of algorithm." Here the "precision of algorithm" means a balance of the precision of the computer calculation and the minute difference of the initial angles between velocity directions for the Lyapunov pair.

In this paper we investigate the quantum mechanical behavior of the Bunimovich stadium and rational billiards. One of our interests lies in how the "precision of algorithm" affects its quantal behavior. It is known that a zero Lyapunov exponent does not necessarily mean that quantal levels are not repulsive.[3, 6] Classically the Lyapunov pair in the pseudointegrable system needs a much longer time to diffuse than in the chaotic system, but it does diffuse. It is reported that diffusion is observed in rational billiards even with a relatively small number of sides.[5] Diffusion is also observed in rhombus billiards[7] even though it has dependence on the "precision of algorithm." This implies that we must carry out calculations up to fairly high energy in order to see the quantal influence of the diffusion in terms of the nearest neighbor level spacing distributions.[7]

This paper is organized as follows. In Section 2 we define the N-stadium which approaches the Bunimovich stadium if N goes to infinity. The method to obtain the eigenenergies and eigenfunctions of these billiards is explained in detail. In Section 3, using several statistics we argue the difference between the Bunimovich stadium and the rational billiards in terms of energy levels. We show that the statistics has an energy dependence, which is easily understood from the uncertainty principle. In Section 4 we study the fourier transformation of the level density, which eventually gives the lengths of classical periodic orbits in each billiard. In Section 5 some wave function in the rational billiard is shown to resemble a scarred wave function appearing in the Bunimovich stadium. In Section 6 we calculate the residual parameter, which is one of the statistics of wave functions. A summary and conclusions are given in Section 7.

2. RATIONAL BILLIARDS AND EIGENFUNCTIONS

A polygonal N-stadium is constructed from the 2×4 stadium of Bunimovich[8] by the following procedure (Fig. 1). Both a and r are equal to one. First part of either the right or left side of the $2N$-sided polygon is inscribed in the corresponding semicircular part of the 2×4 stadium. Then

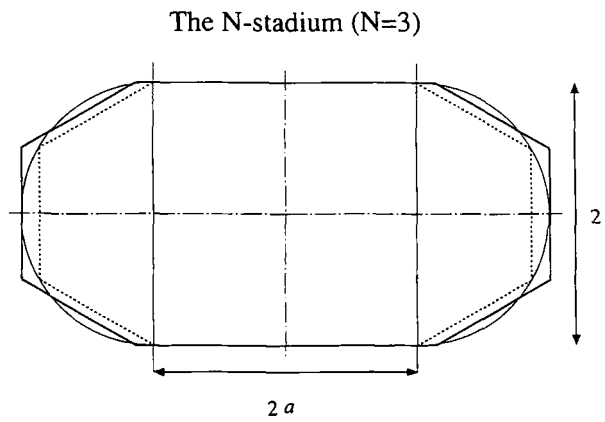

Fig. 1. Schematic illustration of the procedure for making an N-stadium. The dotted lines represent polygons inscribed in the semicircular parts of the 2×4 stadium. We make two horizontal lines longer so that the area of the $2N$-sided polygon remains the same as that of the 2×4 stadium.

we extend two horizontal straight lines to make the area of the $2N$-sided polygon (in fact, now the number of sides is $2N+2$) remain the same as that of the 2×4 stadium ($A=4+\pi$). We call this billiard an N-stadium. The N-stadium with $N\to+\infty$ is considered to be the 2×4 stadium. Half of the vertical height, the parameter r in Fig. 1, remains fixed to one during the above procedure. Therefore we expect that the vertical bouncing ball modes are stable with respect to the change of N. They are indeed found to be very stable in terms both of their energies and the characteristics of wave functions, as one sees later. The areas and the perimeters of the billiards are given in Table I.

In this paper we consider the rational billiards for $N=2, 3, 7, 10$ and the 2×4 stadium billiard and make a comparative study of them. The boundary condition is assumed to be of Dirichlet type. Only the odd–odd wave functions with respect to two symmetry lines are considered. In other

Table I. Areas and Perimeters of the Billiards

Billiard	Area	Perimeter
$N=2$	$4+\pi=7.142$	$\pi+2+4\sqrt{2}=10.798$
$N=3$	$4+\pi$	$\pi+10-\frac{3}{2}\sqrt{3}=10.544$
$N=7$	$4+\pi$	$\pi+4-7\sin(\pi/7)+28\sin(\pi/14)=10.335$
$N=10$	$4+\pi$	$\pi+4-10\sin(\pi/10)+40\sin(\pi/20)=10.309$
2×4 stadium	$4+\pi$	$4+2\pi=10.283$

words we desymmetrize the billiards to avoid degeneracies of even and odd parities with respect to the two symmetry lines. We adopt the time-independent Schrödinger equation:

$$-\frac{h^2}{2m}\Delta\Psi = E\Psi \tag{1}$$

In the following we put $2m=1$ and $h=1$ for simplicity. Then the momentum k and the energy E of the eigenstates are related as $E=k^2$.

To obtain at least a few thousand eigenstates, we use the method of superposition of plane waves, which was invented by Heller.[8] We have checked the accuracy of our calculations by referring to the results given by Heller[8] and Takami[9] in the case of the 2×4 stadium. Our results coincide with theirs, with relative errors less than 10^{-4} in momentum. We have obtained the same eigenenergies as Takami up to the 290th state. In addition we have compared the mode numbers of our results with those given by Weyl's law.[10] Since we consider only the odd–odd eigenstates in our analysis, the desymmetrized billiard has the area $A_q(=1+\pi/4)$ and the perimeter P_q, where the perimeter is $P_q=4+\pi/2$ for the 2×4 stadium and

$$P_q = 3+\frac{\pi}{2}-\frac{N}{2}\sin\left(\frac{\pi}{N}\right)+N\sin\left(\frac{\pi}{2N}\right)+\begin{cases}\cos(\pi/2N) & \text{for } N \text{ odd}\\ 1 & \text{for } N \text{ even}\end{cases} \tag{2}$$

for the N-stadium. Then the mode number by Weyl's law is given by

$$N(E)=\frac{A_q}{4\pi}E-\frac{P_q}{4\pi}\sqrt{E}+\cdots \tag{3}$$

On 2-, 3-, 7-, and 10-stadiums and the 2×4 stadium, 3178, 3172, 3168, 3171, and 3170 eigenenergies are found, respectively, from the ground state up to $k=151$. From the Weyl's law they are estimated as 3168 for the 2-stadium and 3172 for the other billiards. Therefore the numbers almost coincide with those by Weyl's law for $N\geqslant 3$. Some of the figures of the eigenfunctions have been drawn to check that they are indeed the eigenfunctions.

3. ENERGY LEVEL STATISTICS

As will be explained in detail in Section 5, if N is sufficiently large, each eigenfunction of the N-stadium has almost the same structure as the

corresponding one of the 2×4 stadium up to a certain momentum k. Here k depends on N. We call this highest momentum k_N.

The behavior of the nearest neighbor level spacing distribution (NNSD) is dependent on k_N as was already examined on rhombus billiards.[7] In order to take k_N larger, it is expected that we must make N larger. Then the NNSD of the N-stadium becomes indistinguishable from that of the 2×4 stadium. The NNSD up to $k = 151$ shows that the distribution drastically changes when N increases from 2 to 10 (Fig. 2). The NNSD of the 2-stadium seems just in between the Poisson and Wigner distributions. The 2×4 stadium and the 10-stadium look very similar in the NNSD. The Δ_3 statistics for each stadium also shows that upon increasing the number of sides, the shape of the figure shifts from the mixture of Poisson and Wigner distributions to Wigner (Fig. 3). We note here that the Δ_3 statistics of the 2×4 stadium in Fig. 3 is close to that by GOE, but about 10% larger. This may be due to the contribution of the bouncing ball modes.[11, 12]

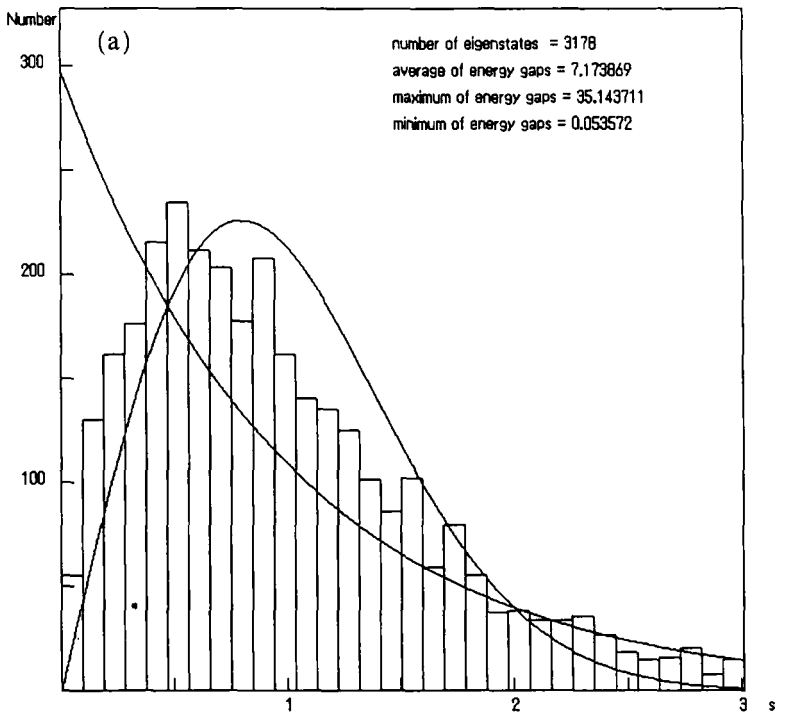

Fig. 2. (a) The NNSD of the 2-stadium. Two solid lines show the Wigner and Poisson distributions. (b) The NNSD of the 3-stadium. (c) The NNSD of the 7-stadium. (d) The NNSD of the 10-stadium. (e) The NNSD of the 2×4-stadium.

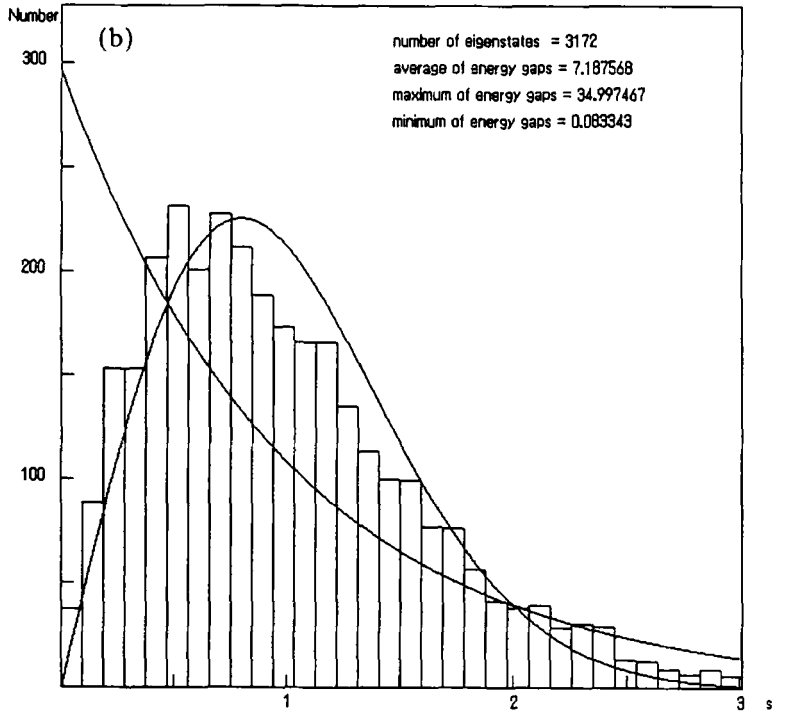

Fig. 2. *(Continued)*

To see the energy dependence of the NNSD, we fit our data to the Brody distribution

$$P_\beta(s) = (1+\beta)\,\alpha s^\beta \exp(-\alpha s^{1+\beta}), \qquad \alpha = \left(\Gamma\left(\frac{2+\beta}{1+\beta}\right)\right)^{1+\beta} \tag{4}$$

where the Brody parameter β is determined by using the method of least squares. The parameters $\beta = 0$ and $\beta = 1$ yield Poisson and Wigner distributions, respectively. It is not our intention to assert that the NNSD is indeed of the Brody type, but our concern is to measure the quantal chaoticity in each billiard. As expected, the fitted Brody parameters have an energy dependence (Fig. 4). From the first excited state each bin of 1000 energy spacings is used to fit the Brody distributions. The distribution of the 2×4 stadium becomes more Wigner-like when the energy gets higher. On the other hand, the 2- and 3-stadiums become more Poisson-like. There is no particular signature for telling the difference between the 10-stadium and the 2×4 stadium in terms of the NNSD below the momentum $k_N = 151$.

Let us express the physical meaning of the above properties of level statistics. As already mentioned, in the low-energy regime eigenfunctions cannot detect the fine structure of the shape of the billiard. At higher

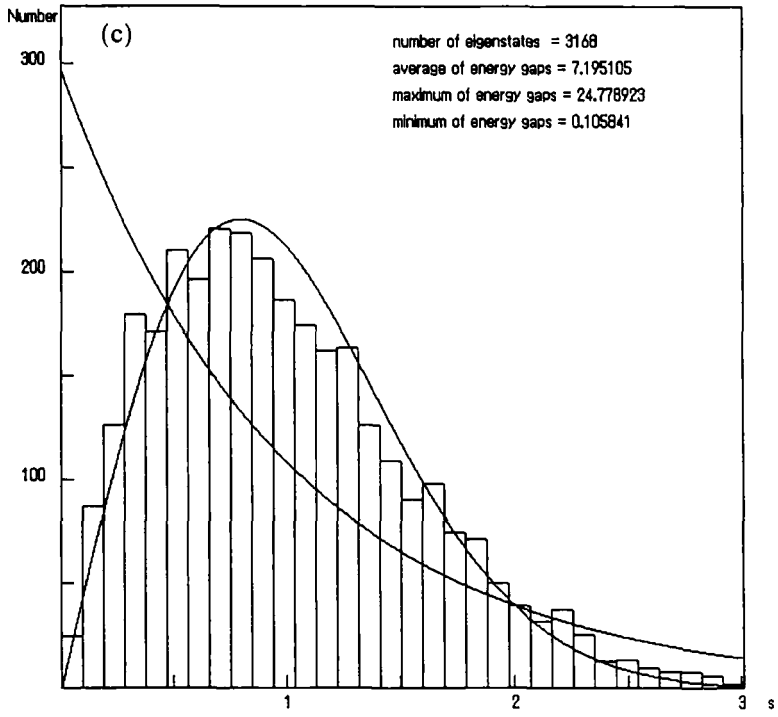

Fig. 2. *(Continued)*

energy, finer structure of the boundary can be realized in terms of the wave functions. From the uncertainty principle, a particle can detect the difference of the shape l if its size is comparable to the wavelength

$$l \approx \lambda = \frac{h}{mk} = \frac{2}{k} \tag{5}$$

We have $l \approx 0.01$ for $k = 151$. Roughly speaking, the difference between both shapes is caused by the replacement of semicircles by polygons. The farthest point on the perimeter of the 2×4 stadium from the corresponding one on the N-stadium has a distance of the same order (see Fig. 1),

$$l \approx 1 - \cos\left(\frac{\pi}{2N}\right) \approx \frac{\pi^2}{8N^2} \tag{6}$$

If $N = 10$, the distance is in the order of 0.01. This justifies our numerical experiment on the energy level statistics. It is found that $\beta_\infty - \beta_N$ is proportional to $1/N^2$ as shown in Fig. 5, where β_∞ is the fitted Brody parameter for the 2×4 stadium and β_N is that for the N-stadium. A similar relation between N and the initial velocity angular separation in classical mechanics was already reported.[5]

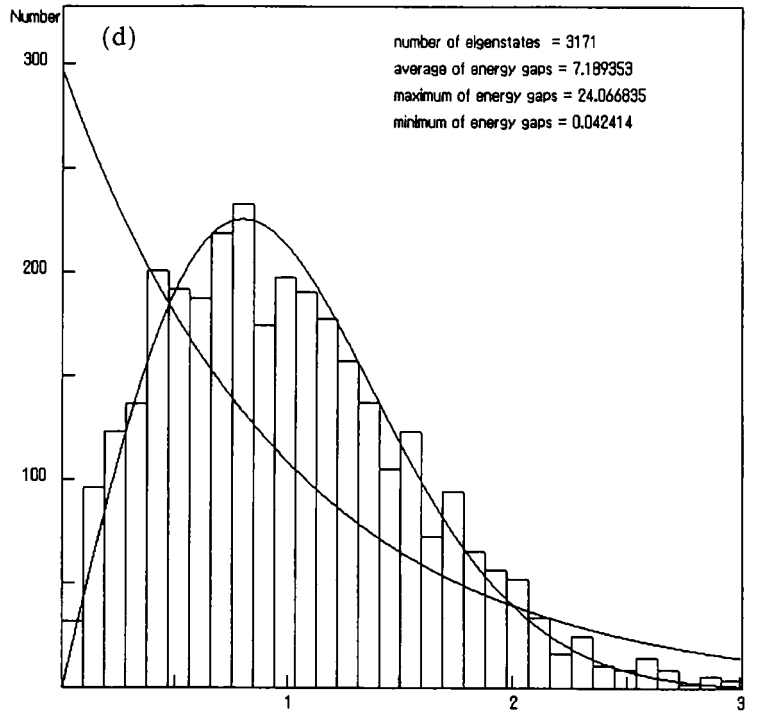

Fig. 2. *(Continued)*

4. FOURIER TRANSFORMATION OF LEVEL DENSITY AND PERIODIC ORBITS

Since the invention of the trace formula by Gutzwiller, it has been known that each peak of the Fourier transformation of the level density corresponds to a (or one-parameter family of) classical periodic orbit both in regular and chaotic systems. In rational billiards most of the peaks come from the stable bouncing ball mode orbits, but they come from isolated unstable periodic orbits in the 2×4 stadium. By inspection we find the classical periodic orbits up to the length $L = 14$ for the 2-stadium (Fig. 6) and up to $L = 8$ for the 3-stadium (Fig. 7).

Fourier transformation of the level density (with respect to momentum) is defined as

$$\tilde{d}(L) = \int_0^\infty dk \exp(ikL) \sum_{j=1}^{J} \delta(k^2 - k_j^2) = \sum_{j=1}^{J} \frac{\exp(ik_j L)}{2k_j} \tag{7}$$

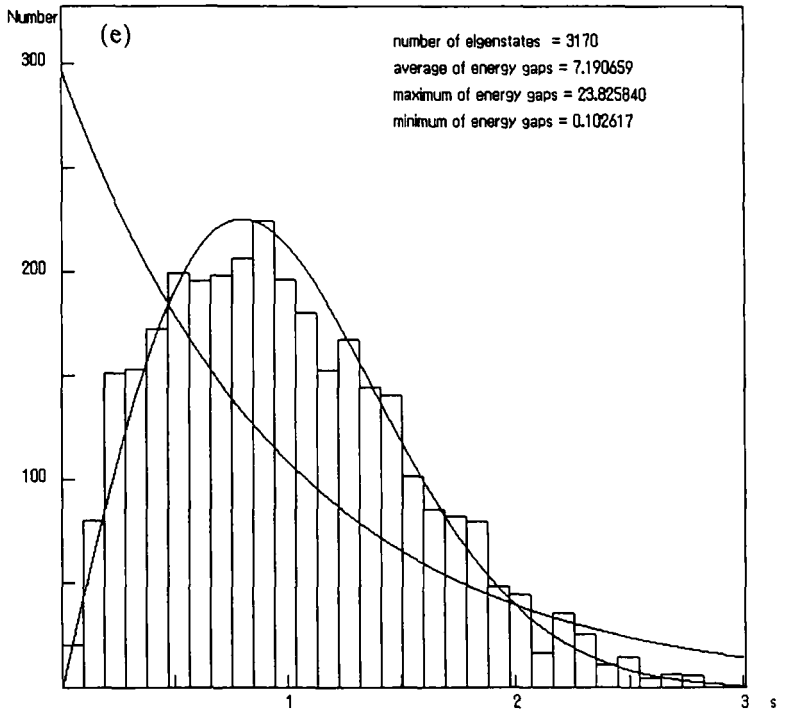

Fig. 2. *(Continued)*

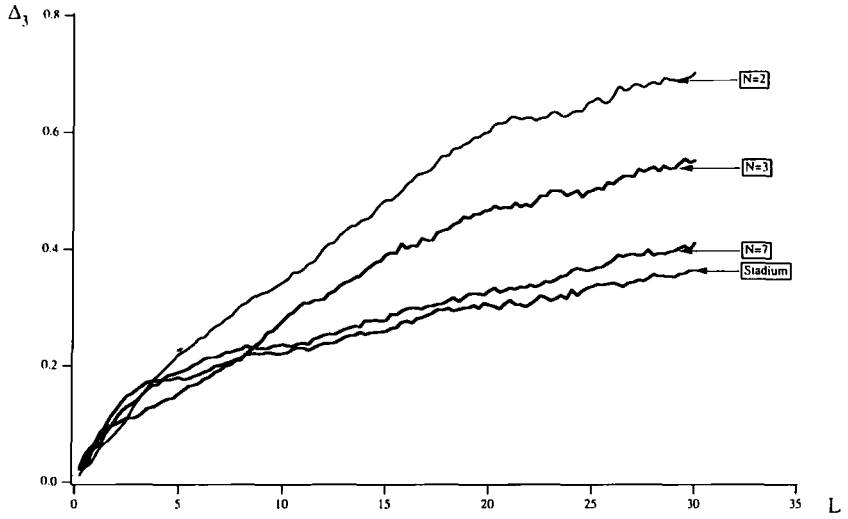

Fig. 3. The Δ_3 statistics of the N-stadium ($N = 2, 3, 7$) and the 2×4 stadium.

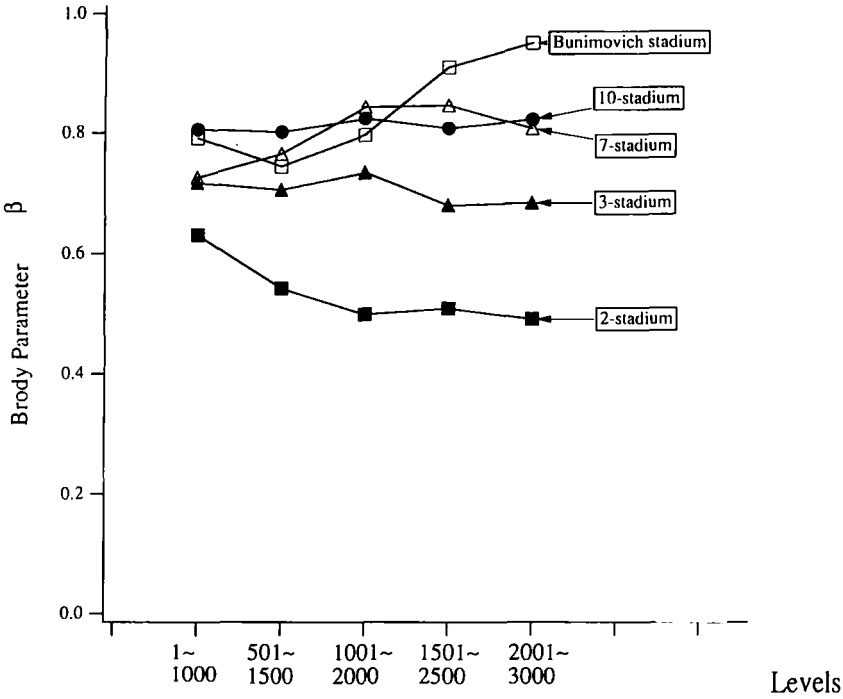

Fig. 4. Energy dependence of the Brody parameter of the N-stadium ($n = 2, 3, 7, 10$) and the 2×4 stadium.

where k_j is the momentum of the jth level and k_J is the momentum of the highest eigenstate we consider. In Fig. 8a–8e we show the $|\tilde{d}(L)|^2$ of the 2-, 3-, 7-, and 10-stadiums and the 2×4 stadium, respectively.

The N-stadium has unique peaks coming from the vertical bouncing ball modes ($L = 2.0, 4.0, 6.0, \ldots$) which also exist in the 2×4 stadium. In the N-stadium most of the peaks essentially correspond to bouncing ball modes of one-parameter families of periodic orbits. The only exception we find in the 2-stadium is the periodic orbit with $L = 4.65$. It is an isolated closed orbit of length 4.65 in a family of length 9.29 (Fig. 6a) in the special condition that the trajectory must cross just at the center of the horizontal straight lines. It is considered as the special case of a one-parameter family of stable periodic orbits. It may be called an "unstable" orbit. Its triple $L = 13.95$ also can be seen as a peak.

In the 3-stadium we must have peaks of horizontal bouncing ball modes ($L = 4.004, 8.008, \ldots$), but they happen to be very close to the

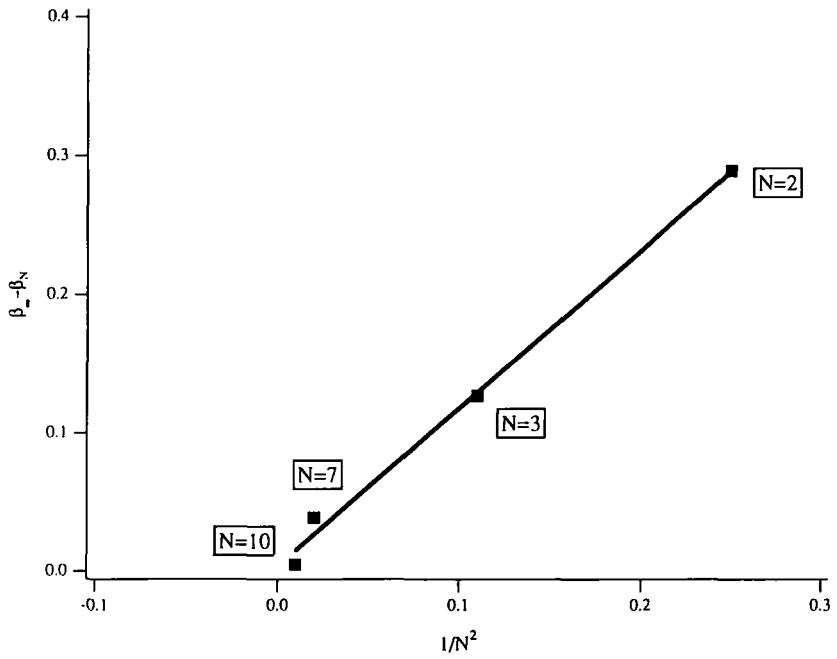

Fig. 5. $\beta_{\infty} - \beta_N$ as a function of $1/N^2$.

vertical ones ($L = 4.0, 8.0, \ldots$). Therefore horizontal bouncing modes are obscured by these vertical ones. Several "unstable" orbits are also found ($L = 4.60, 4.87, 6.33$; cf. Fig. 7).

Fourier transformation of the 10-stadium with $k_J = k_N$ is also very similar to that of the 2×4 stadium. In the 2×4 stadium it is known[13] that each peak corresponds to a classical (unstable, isolated) periodic orbit (Fig. 8e) (length of 2.0, 4.0, 4.47, 4.83, 5.0, 5.14, 5.20, 5.66, 6.00, 6.47, etc.). The corresponding peaks are clearly seen in the 10-stadium.

5. SCARS IN CHAOTIC- AND RATIONAL- BILLIARDS

The eigenfunction of $k_i (\leqslant k_N)$ does not detect the precise structure of the peripheral part, that is, it does not detect whether the wave in the billiard is reflected by the semicircular part or the polygonal one. This means that in spite of its rationality a wave-function of the N-stadium might have "scars" of classical periodic orbits, which is a characteristic feature for chaotic systems. It is rather astonishing if we consider that the classical periodic orbits are very delicate with respect to reflection angles.

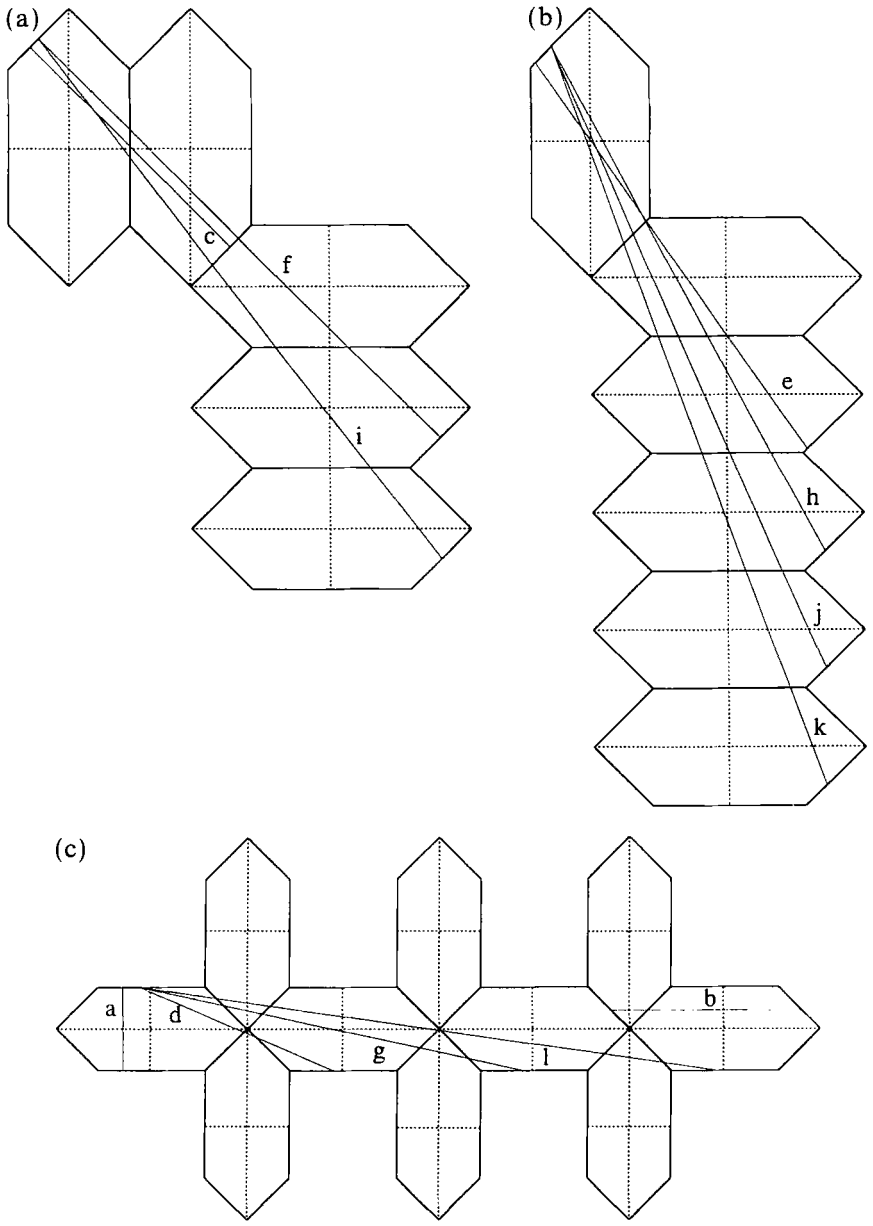

Fig. 6. Principal periodic orbits of the 2-stadium. Dotted lines represent the symmetry lines of the 2-stadium. The orbit c is an isolated "unstable" orbit $L = 4.65$. Others are representative of the one-parameter families of periodic orbits $L = 2.00$ (a), 4.57 (b), 5.00 (d), 8.01 (e), 9.29 (f), 9.36 (g), 9.71 (h), 10.80 (i), 11.52 (j), 13.38 (k), 13.86 (l).

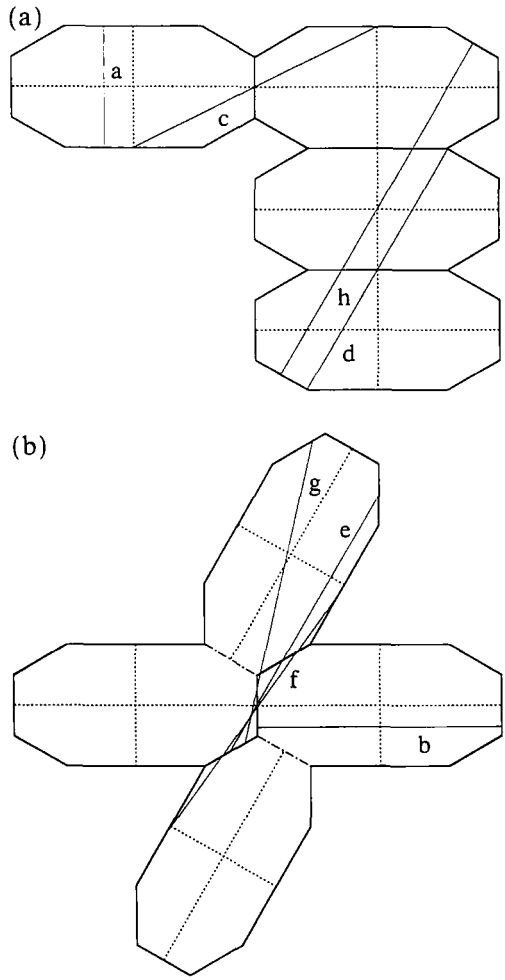

Fig. 7. Principal periodic orbits of the 3-stadium. Dotted lines represent the symmetry lines of the 3-stadium. The 3-stadiums are not pasted at broken lines. The orbits d, e, and h are isolated "unstable" orbits $L = 4.60, 4.87$, and 6.33, respectively. Others are representatives of the one-parameter families of periodicorbits $L = 2.00$ (a), 4.00 (b), 4.48 (c), 4.90 (f), 5.10 (g).

The nodal pattern of wave functions also supports our observation (Figs. 9–12). We calculate squared absolute values of eigenfunctions to see the nodal pattern. As expected, vertical bouncing ball modes often appear in the rational billiards. The wave functions of the 10-stadium and corresponding ones of the 2×4 stadium look very alike. In the 10-stadium even the scarred wave functions exist at expected eigenenergies. For

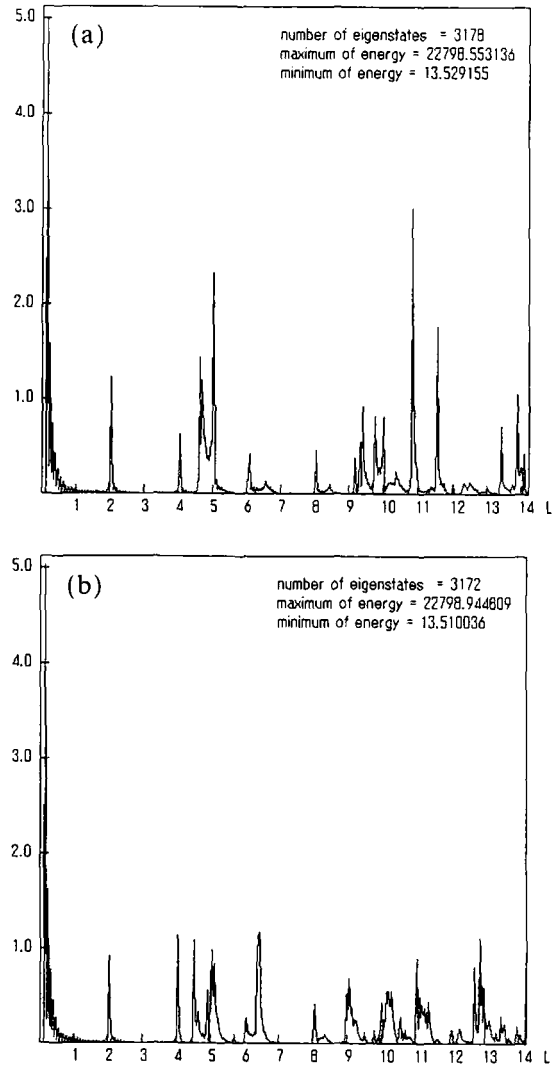

Fig. 8. (a) Fourier transform of the spectrum of the 2-stadium. (b) Fourier transform of the spectrum of the 3-stadium. (c) Fourier transform of the spectrum of the 7-stadium. (d) Fournier transform of the spectrum of the 10-stadium. (e) Fourier transform of the spectrum of the 2×4 stadium.

example, compare the $\#431(k = 56.7659)$ of the 2×4 stadium (Fig. 9a) and the $\#433(k = 56.8016)$ of the 10-stadium (Fig. 10a).

The wave functions of the 2-stadium usually look similar to integrable ones. They have some regular and repeated patterns (Fig. 11a–11h).

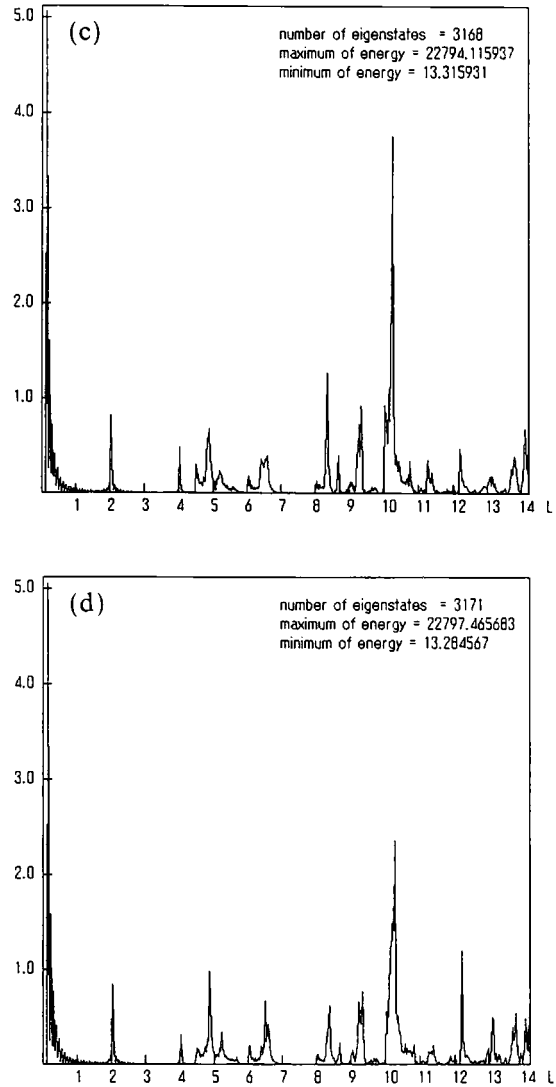

Fig. 8. *(Continued)*

Mainly the vertical and oblique ($\pi/4$ with respect to a horizontal line) bouncing ball orbits contribute to those regular nodal patterns. The wave functions with irregular patterns must be affected by some orbits with longer periods. The orbit of period 4.65 cannot be seen as a "scar" in the

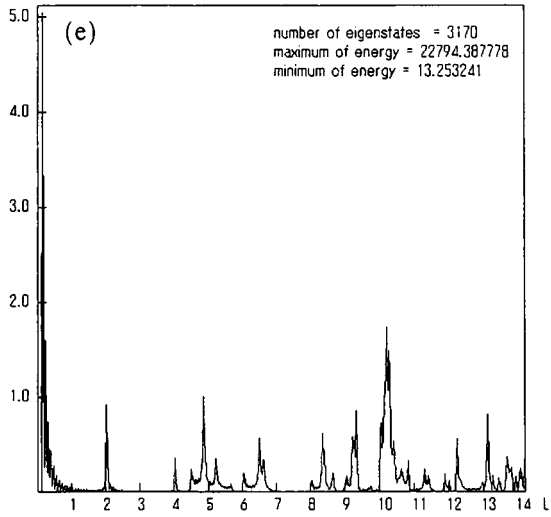

Fig. 8. *(Continued)*

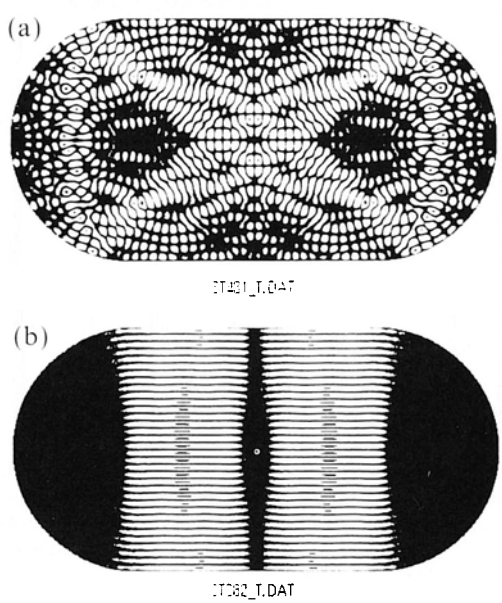

Fig. 9. (a) #431 in the 2×4 stadium with $k = 56.7659$. (b) #382 in the 2×4 stadium with $k = 53.4741$.

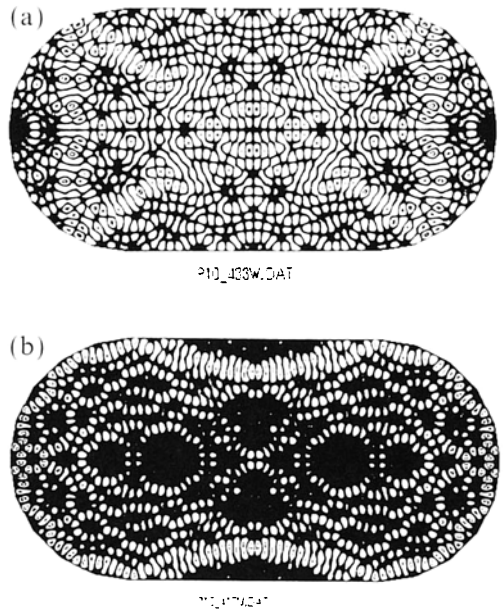

Fig. 10. (a) #433 in the 10-stadium with $k = 56.8016$. (b) #417 in the 10-stadium with $k = 55.7383$.

wave functions. It is obscured by the overwhelming contributions of the family of $L = 9.29$. By this graphical method it is confirmed that the 3-stadium also has horizontal bouncing ball modes (Fig. 12b, 12g) in addition to the vertical ones.

If we take $k \leqslant 151$, it is numerically observed that we can approximate the 2×4 stadium by the rational billiards with $N \geqslant 10$. Therefore in the analysis of wave functions we arrive at the same condition of the "uncertainty principle" discussed in Section 3. The granulation of the wave functions is at the smallest of the order of the wavelength λ, as seen from the figures. The fine structure of the boundaries, which is much smaller than the wavelength, does not seriously affect the properties of the wave functions.

6. THE RESIDUAL PARAMETER

Several statistical properties of wave functions have also been invented to measure their chaotic features.[14, 15] The amplitude distribution $P(\psi)$ is

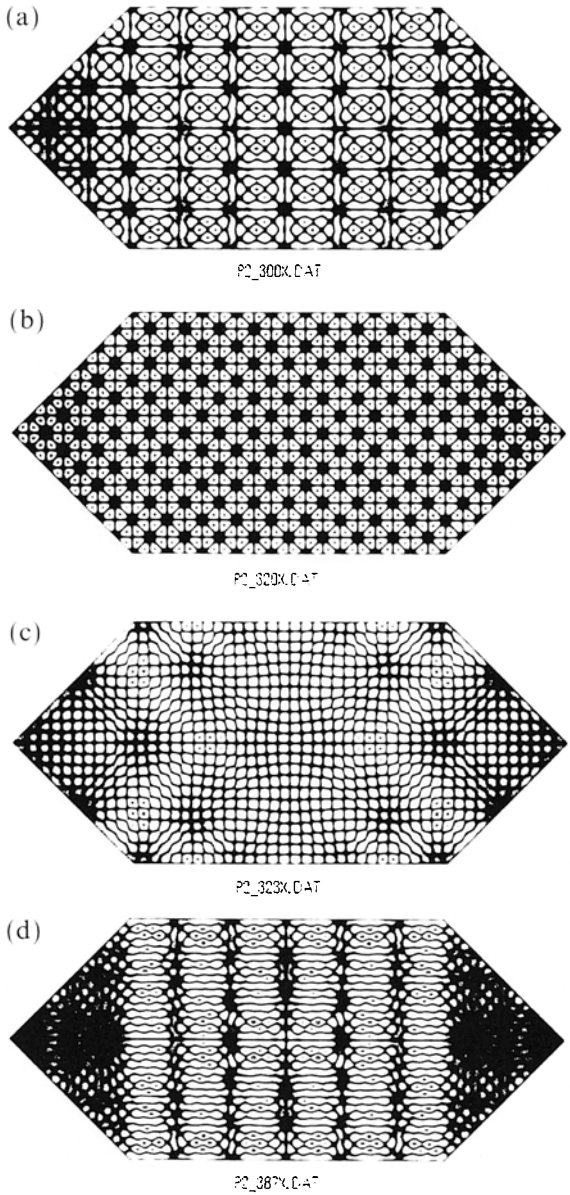

Fig. 11. (a) #300 in the 2-stadium with $k = 47.6843$; (b) #320 in the 2-stadium with $k = 49.1781$; (c) #323 in the 2-stadium with $k = 49.3633$. (d) #387 in the 2-stadium with $k = 53.8502$. (e) #420 in the 2-stadium with $k = 56.1681$. (f) #456 in the 2-stadium with $k = 58.3162$. (g) #468 in the 2-stadium with $k = 59.1898$; (h) #473 in the 2-stadium with $k = 59.4244$; (i) #314 in the 2-stadium with $k = 48.6303$.

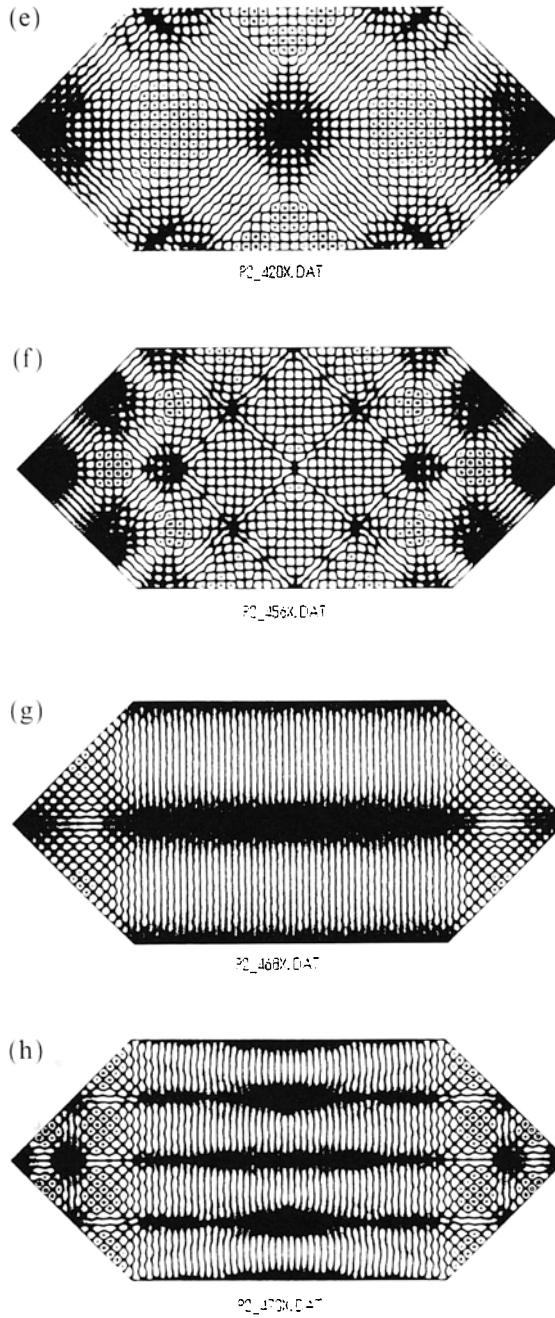

Fig. 11. *(Continued)*

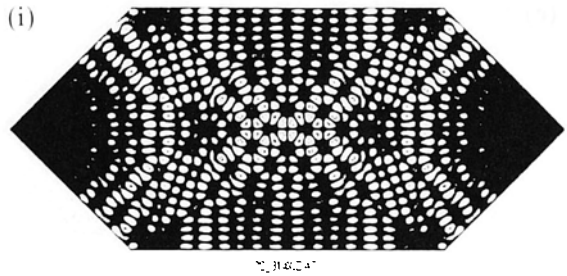

Fig. 11. *(Continued)*

the probability of finding the value Ψ of the wave function. In chaotic billiards it is expected to form the Gaussian distribution

$$P_G(\psi) = \left(\frac{A}{2\pi}\right)^{1/2} \exp\left(-\frac{A}{2}\psi^2\right) \tag{8}$$

where A is the area of the billiards.[14-16] In two-dimensional rectangular billiards, which are integrable, it has a different form,[17]

$$P_R(\psi) = \begin{cases} \dfrac{4\sqrt{A}}{\pi(2+\sqrt{A}\,|\psi|)} K\left(\dfrac{2-\sqrt{A}\,|\psi|}{2+\sqrt{A}\,|\psi|}\right), & 0 \leqslant |\psi| \leqslant \left(\dfrac{4}{A}\right)^{1/2} \\ 0 & \text{otherwise} \end{cases} \tag{9}$$

where $K(x)$ is the complete elliptic integral of the first kind. The wave functions of the rectangular billiards always display periodic texture. Therefore, in order to distinguish between chaotic and integrable billiards, we adopt the residual parameter,[15, 17] which is defined as

$$\rho^2 = \int d\psi \, (P(\psi) - P_G(\psi))^2 \tag{10}$$

It measures the deviation from the Gausssian distribution $P_G(\psi)$. We calculate ρ^2 from the ground state to the 500th state for each billiard. The integration is done numerically by selecting at random 10000 points inside the billiards. Results are shown in Fig. 13. Near the ground state $P(\psi)$ is far from the Gaussian distribution, but generally ρ^2 becomes smaller when the energy gets higher.

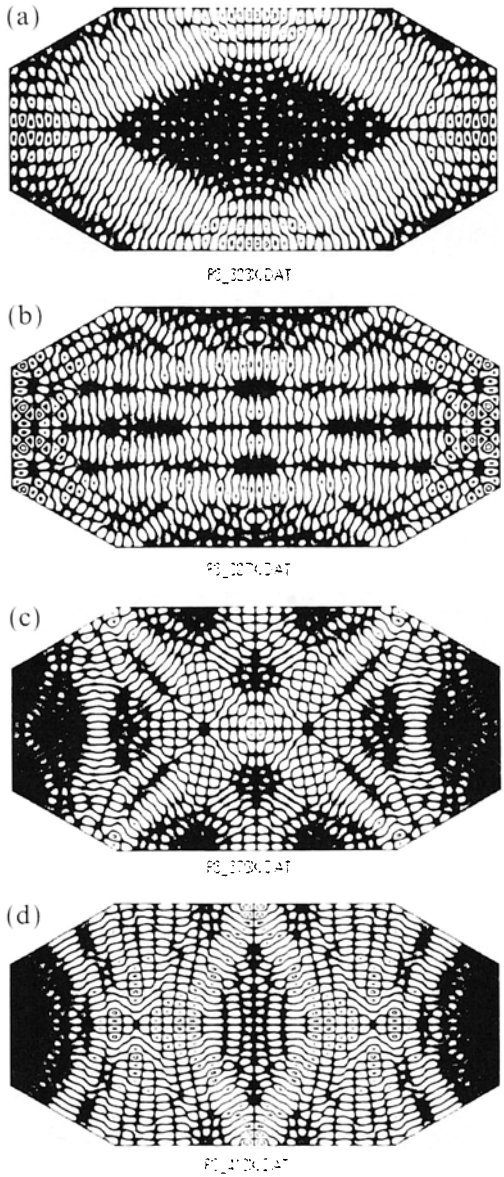

Fig. 12. (a) #323 in the 3-stadium with $k = 49.2341$; (b) #327 in the 3-stadium with $k = 49.6097$; (c) #370 in the 3-stadium with $k = 52.6534$; (d) #413 in the 3-stadium with $k = 55.5165$; (e) #433 in the 3-stadium with $k = 56.7933$; (f) #445 in the 3-stadium with $k = 57.6032$; (g) #457 in the 3-stadium with $k = 58.2706$.

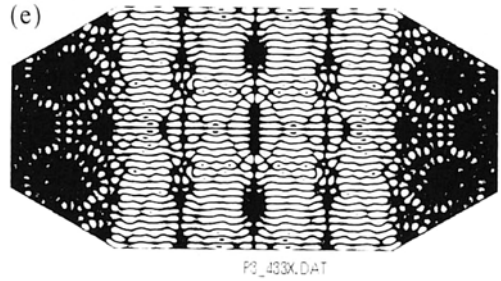

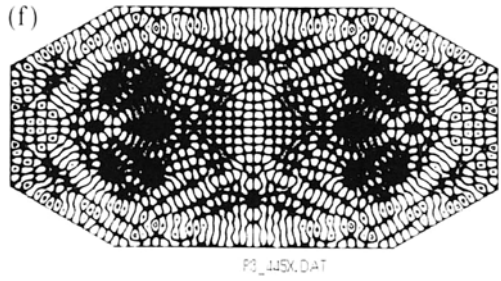

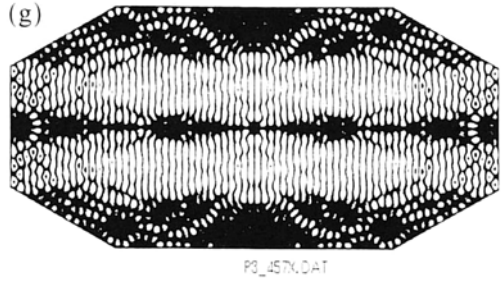

Fig. 12. *(Continued)*

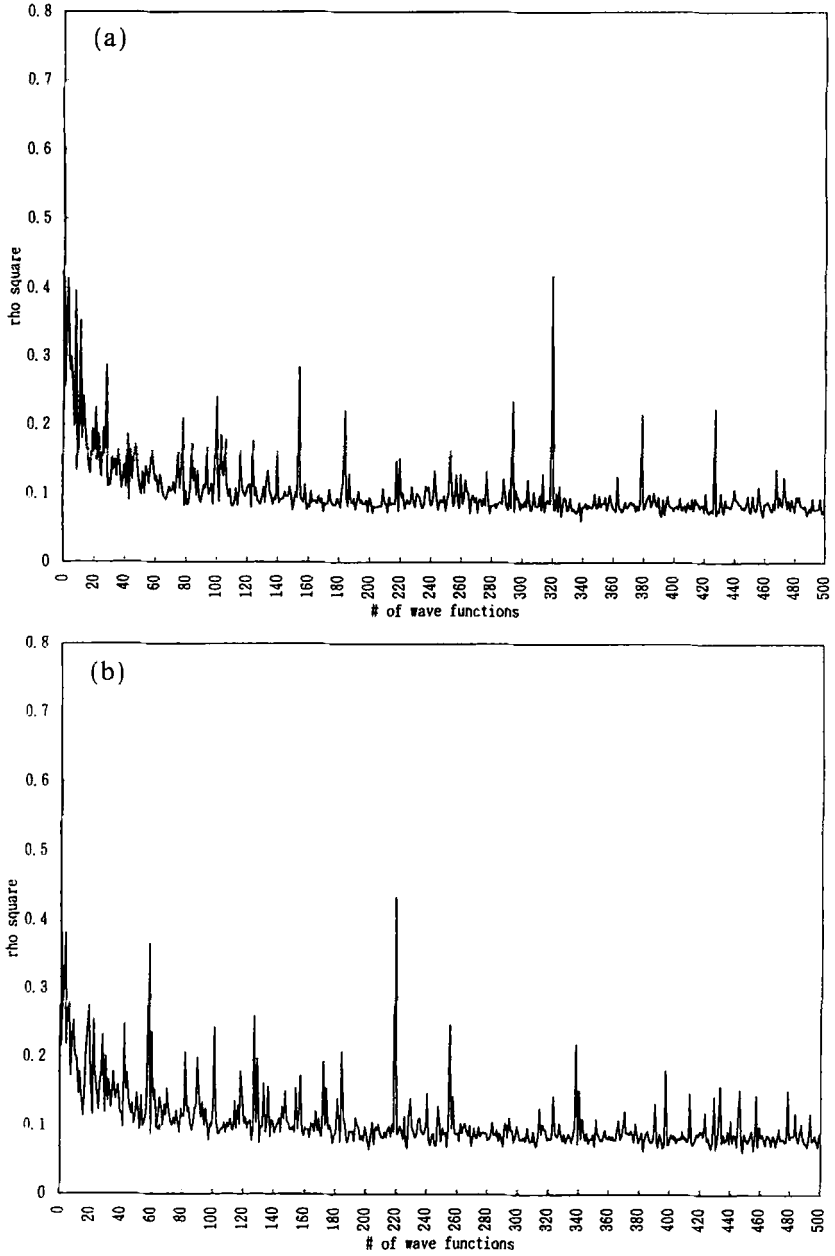

Fig. 13. (a) The residual parameter ρ^2 for the 2-stadium from the ground state to the 500th state; (b) the same for the 3-stadium; (c) the same for the 7-stadium; (d) the same for the 10-stadium; (e) the same for the 2×4 stadium.

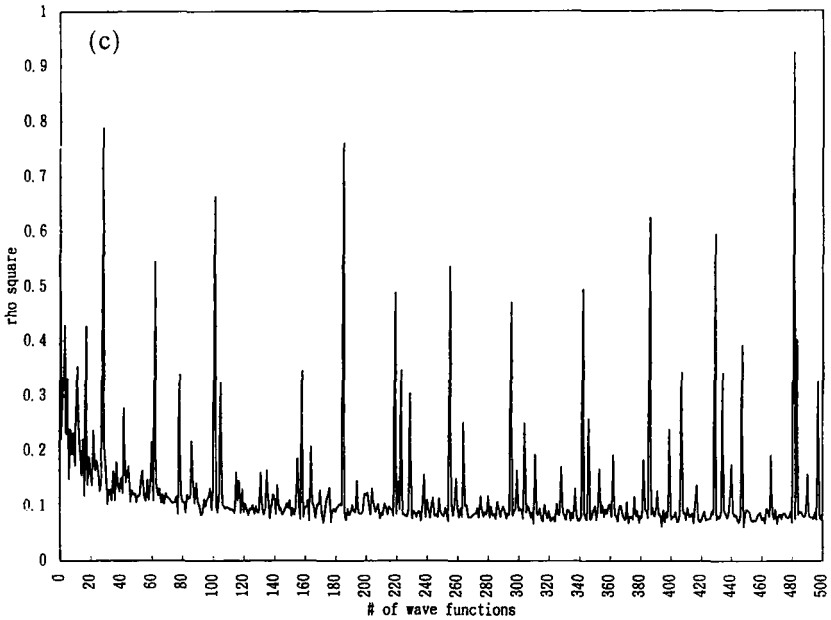

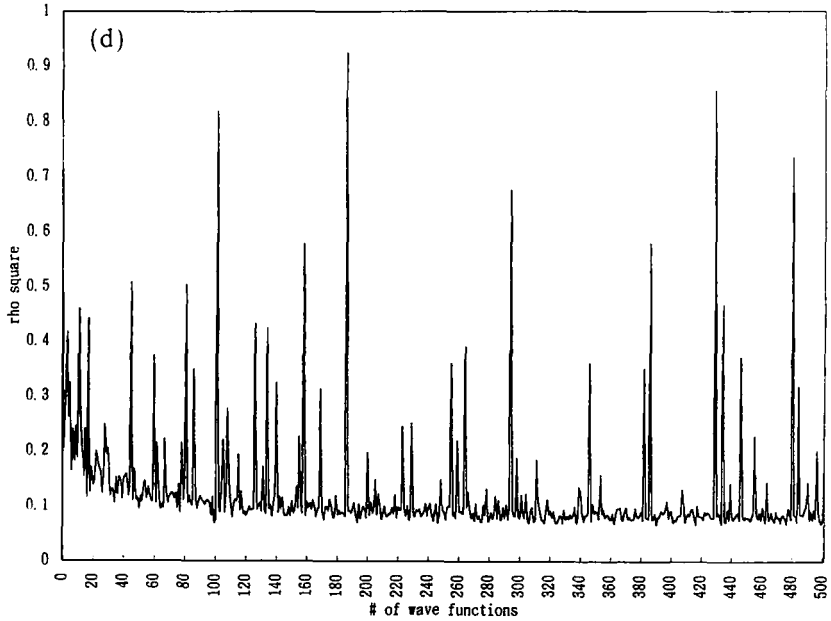

Fig. 13. *(Continued)*

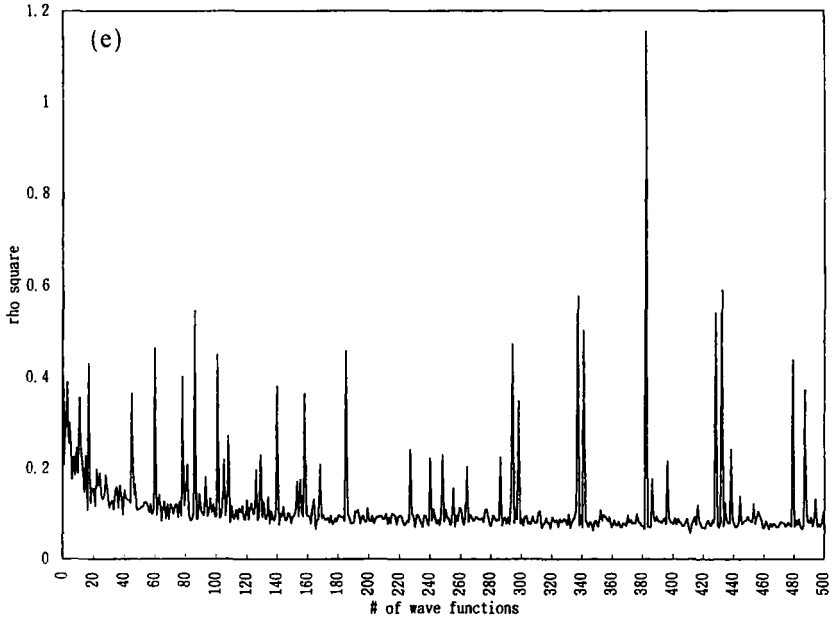

Fig. 13. *(Continued)*

There are some individual wave functions which have relatively high ρ^2 values. Most of the high peaks in Fig. 13 correspond to the bouncing ball modes for any billiard. In the 2×4 stadium the only exception is a whispering gallery mode $\#153(k=34.5330)$ where $\rho^2=0.170$. Although we find several scarred wave functions, they do not appear as any significant peaks in Fig. 13e. Therefore it is hard to find a scarred wave function only from the value of the residual parameter. For example, $\#431$ $(k=56.7659)$ of the 2×4 stadium (Fig. 9a) has a very small ρ^2 $(=0.081)$, but it has a scar.

The peaks in the 2- and 3-stadiums are generally smaller than those in the 2×4 stadium. This is because in the 2×4 stadium bouncing ball modes are distinct; on the other hand in the 2- and 3-stadiums bouncing ball modes are obscured due to the contribution of the same one-parameter families of periodic orbits (cf. Fig. 11d, 12e, and 9b).

In the 2-stadium, there exist not only vertical ones which are already seen in the 2×4 stadium, but also $\pi/4$ directed bouncing ball modes (Fig. 11c, 11e, 11f). Some wave functions almost vanish at the right-angle corner. This makes ρ^2 a little larger. For instance, $\#314$ $(k=48.6303)$ has $\rho^2=0.128$ (Fig. 11i). A large number of wave functions have pseudoperiodic

textures (for example, #300, Fig. 11a), but their ρ^2 are not particularly large ($\rho^2 = 0.086$ for #300). The only exception is #320 (Fig. 11b), which gives a most impressive example. It has very large $\rho^2 (= 0.417)$ and gives an almost perfect periodic pattern.

In the 3-stadium there exist fewer bouncing ball modes and smaller values of the ρ^2 peaks than in the 2-stadium. The pseudoperiodic texture is not seen in the 3-stadium. It has more varieties of one-parameter families of periodic orbits including horizontal bouncing ball modes (Fig. 12). For $L \leqslant 8$ we have seven principal periodic orbits in the 3-stadium ($L = 2.00, 4.48, 4.60, 4.87, 4.90, 5.10, 6.33$), but only four in the 2-stadium ($L = 2.00, 4.58, 4.65, 5.00$). Therefore the wave function behavior may become more complicated in the 3-stadium.

In the 10-stadium, at least in studying the behavior of the wave-function and the residual parameter, no difference from the 2×4 stadium can be found. We find many bouncing ball modes, scarred states (see, Fig. 10a) and a few whispering gallery modes (Fig. 10b). The ρ^2's are relatively larger than other stadiums, but this may depend on the accuracy of the wave functions which we calculate. The statistics of wave functions seems more sensitive to the accuracy of our calculation than that of spectroscopy.

7. SUMMARY AND CONCLUDING REMARKS

In this paper we have investigated numerically the 2×4 stadium and the 2- 3- 7- and 10-rational billiards. About 3170 levels from the ground state are calculated for each billiard. It is numerically observed that the rational N-stadium has a tendency to ergodicity when $N \to +\infty$. The NNSD changes from the Poisson-like statistics to Wigner-like statistics as the number of sides increases from 2 to 10, which is indicated by the fitted Brody parameter β. The higher the energy, the more distinct is the difference between the pseudointegrable billiard and the chaotic one. The Δ_3 statistics also shows a similar change. Our calculation also shows the energy dependence of the fitted Brody parameter. Each peak in the Fourier transformation of the energy spectra corresponds to a classical periodic orbit. In rational billiards almost all of the orbits are found to correspond to stable bouncing ball orbits.

The tendency to ergodicity in level statistics is also confirmed by the behavior of the wave functions. Up to $k = 151$ the wave functions in the 10-stadium and the corresponding ones in the 2×4 stadium look very alike.

Although it is believed that the rational billiards have no metric entropy, the situation is quite different in quantum mechanics. If the

difference of shape between the 2×4 stadium and the rational billiards is less than the wavelength, we cannot tell the difference in terms of the wave functions and energy level statistics.

In the case of $N = 2$, similar observations have already been made.[3, 18] In ref. 18 several parameters were examined. Although topologically all these are genus-2 billiards, the NNSD and the Δ_3 statistics vary with the parameters. The genus number is an important factor, but geometrical factors, i.e., lengths of boundary segments, angles of corners, etc., are also key issues to determine the characteristics of spectral statistics.

If we wish to know the difference in the shapes of billiards using a Lyapunov pair with velocity v, the inequality $v\,T \cdot \alpha > \text{const}\ 1/N^2$ should hold, where α is the initial velocity angular separation and T is the elapsed time. The argument that the difference of shape is of the order of $1/N^2$ is assumed here. Therefore, setting $\alpha N^2 = \text{const}$, we find that the classical behavior of the rational billiards looks similar with respect to the Lyapunov exponent.[5] However, all of these are numerical results. Analytical support is necessary to make our conclusions more definite.

ACKNOWLEDGMENT

One of the authors (N.Y.) would like to express his gratitude to Riken where a part of this work has been done using the supercomputer VPP500.

REFERENCES

1. M. V. Berry, In *Semiclassical Mechanics Regular and Irregular Motion* (Les Houches, Session XXXVI, 1981), G. Iooss, R. H. G. Helleman, and R. Stora, eds. (North-Holland, Amsterdam, 1983), p. 171.
2. A. N. Zemlyalov and A. B. Katoh, *Math Notes* **18**:760 (1976); **20**:1051 (1976).
3. P. J. Richens and M. V. Berry, *Physica D* **2**:495 (1981).
4. B. Eckhardt, J. Ford, and F. Vivaldi, *Physica D* **13**:329 (1984).
5. J. L. Vega, T. Uzer and J. Ford, *Phys. Rev. E* **48**:3414 (1993).
6. T. Cheon and T. D. Cohen, *Phys. Rev. Lett.* **62**:1769 (1989).
7. A. Shudo and Y. Shimizu, *Phys. Rev. E* **47**:54 (1993).
8. E. Heller, in *Wavepacket Dynamics and Quantum Chaology* (Les Houches Summer School. Session LII, 1989), M.-J. Giannoni, A. Voros and J. Zinn-Justin, eds. (North-Holland, Amsterdam, 1991), p. 547.
9. T. Takami, *Phys. Rev. Lett.* **68**:3371 (1992).
10. H. P. Baltes, and E. R. Hilf, *Spectra of Finite Systems* (BI Wissenschaftsverlag, Mannheim, 1976).
11. H.-D. Gröf, H. L. Harney, H. Lengeler, C. H. Lewenkopf, C. Rangacharyulu, A. Richter, P. Schardt, and H. A. Weidenmüller, *Phys. Rev. Lett.* **69**:1296 (1992).
12. M. Sieber, U. Smilansky, S. C. Creagh, and R. G. Littlejohn, *J. Phys. A: Math. Gen.* **26**:6217 (1993).
13. E. B. Bogomolny, *Physica D* **31**:169 (1988).

14. S. W. McDonald and A. N. Kaufman, *Phys. Rev. A* **37**:3067 (1988).
15. Y. Shimizu and A. Shudo, *Prog. Theor. Phys. Suppl.* **116**:267 (1994).
16. P. Seba, *Phys. Rev. Lett.* **64**:1855 (1990).
17. T. Shigehara, *Phys. Rev. E* **50**:4357 (1994).
18. A. Shudo and Y. Shimizu, Statistical properties of eigen-functions for quantum billiards with and without positive exponent, to be published.